

Frequency-Modulated Continuous-Wave Coherent Lidar With Downlink Communications Capability

Zhongyang Xu, Kai Chen¹, Xiuyuan Sun, Kelin Zhang, Yicheng Wang, Jie Deng,
and Shilong Pan¹, *Senior Member, IEEE*

Abstract—A frequency-modulated continuous-wave (FMCW) coherent lidar with downlink communication capability is proposed based on phase-diversity coherent detection, by which laser ranging, laser velocimetry and free-space optical downlink communications can be simultaneously achieved. In the local transceiver, a linear-frequency modulated (LFM) optical signal is generated and used as the lidar signal. The LFM optical signal is received by the remote transceiver and coded with data via amplitude modulation. Then, the light is transmitted back to the local transceiver, in which a phase-diversity coherent optical receiver is used to simultaneously extract the range, velocity, and communication data. The in-phase and quadrature outputs from the phase-diversity coherent optical receiver are simultaneously recorded to reform a complex signal. The data is extracted from the intensity of the complex signal, while the range and velocity are obtained from the argument of it. A demonstration experiment is carried out. Different digital baseband signals are encoded on the reflected signal via an intensity modulator, while the 80-MHz Doppler frequency shift is simulated by an acousto-optic modulator. The impact of the digital signal on lidar detection is removed. Meanwhile, the communication quality is little affected by the varied frequency of the de-chirped signal. Therefore, the lidar detection and the free-space optical communications are simultaneously implemented.

Index Terms—Lidar, free-space optical communications, phase-diversity coherent detection.

I. INTRODUCTION

AS A combination of radar and laser technology, lidar has been widely used in many areas since its early applications in the 1960s [1]. However, in many applications such as satellite laser ranging [2], remote sensing [3], and automatic navigation [4], a single-functional lidar system is insufficient. Lidar systems with multiple functions such as tracking [5], monitoring [6], localization [7], and navigation [8] are required. For instance, in automatic navigation, not only lidar detection but also the communications between vehicles is required to share the locations or traffic conditions [9], [10]. A lidar system with communication capability is highly desired and promising for automotive driving [11],

satellite networks [12], and large-scale facilities [13]. Recently, lidar systems with communication capability have been proposed based on pseudo-random noise (PRN) sequences [13]. Self-correlation of PRN sequences is used to measure the range in the period of laser ranging. Meanwhile, the optical PRN sequences are coded with data for free-space optical (FSO) communications. Since time-division multiplexing is used, the laser ranging and communications are respectively implemented in different time slots. However, the method is difficult to be applied in automatic driving and navigation, in which a pulsed lidar are usually used. Since the pulsed lidars usually transmit low-duty-cycle optical pulses so that it is difficult to encode the high bit-rate data on the lidar signals.

Frequency-modulated continuous-wave (FMCW) lidar is another kind of widely-used lidars [14], which has the advantages of low peak power, large dynamic range, and high ranging resolution [15]. Different from pulsed lidars, FMCW lidars transmit continuous lightwave so that the high bit-rate data can be encoded on the lidar signals, which promises an FMCW lidar system with communication capability. Although multiple functions have been enabled on FMCW lidar systems using various advanced schemes of signal detection and processing [16]–[18], different functions may have negative impacts on each other. For example, in an FMCW lidar system with communication capability, the existence of digital signals may affect the waveforms of linear-frequency-modulated (LFM) optical signals. In extreme cases, the laser ranging might be disabled since the real-time waveforms are severely changed. On the other hand, since LFM optical signals are used in the FMCW lidar, the frequency of the optical carrier is varied so that the coherent FSO communications may be influenced.

In this letter, we propose an FMCW lidar with the downlink communications capability based on a phase-diversity coherent optical receiver, which has been preliminarily demonstrated in our previous letter [19]. The phase-diversity coherent detection can simultaneously extract the intensity and phase of the signal so that an additional degree of freedom can be used to develop a multifunctional lidar. In the local transceiver, an LFM optical signal is generated and transmitted to the remote transceiver. The LFM lightwave is coded by a digital baseband signal via amplitude modulation in the remote transceiver. Then, the coded lightwave is transmitted back to the local transceiver, which is detected with a phase-diversity coherent optical receiver. A proof-of-concept experiment is carried out, in which an FMCW lidar with downlink communication capability is demonstrated. The results show that laser ranging is still feasible even though the LFM lightwave is obviously changed by the digital baseband signal. Meanwhile, the data is little influenced by the varied optical carrier and

Manuscript received March 27, 2020; revised April 9, 2020; accepted April 21, 2020. Date of publication April 28, 2020; date of current version May 12, 2020. This work was supported in part by NSFC Program under Grant 61605190, in part by the Shanghai Academy of Spaceflight Technology (SAST) Innovation Fund under Grant SAST2018054, in part by the Jiangsu Provincial 333 Project under Grant BRA2018042, and in part by the Fundamental Research Funds for Central Universities. (*Corresponding author: Shilong Pan.*)

The authors are with the Key Laboratory of Radar Imaging and Microwave Photonics, Ministry of Education, Nanjing University of Aeronautics and Astronautics, Nanjing 210016, China (e-mail: pans@nuaa.edu.cn).

Color versions of one or more of the figures in this letter are available online at <http://ieeexplore.ieee.org>.

Digital Object Identifier 10.1109/LPT.2020.2990942

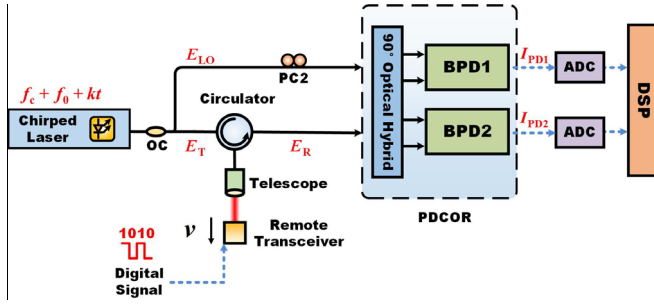


Fig. 1. Schematic diagram of the FMCW lidar with downlink communication capability. The solid black lines are optical fibers and the dashed blue lines are electrical cables; OC: optical coupler; PC: polarization controller; PDCOR: phase-diversity coherent optical receiver; BPD: balanced photodetector; ADC: analog-to-digital converter; DSP: digital signal processor.

the optical Doppler frequency shift (DFS). Therefore, the range, velocity, and communication data can be simultaneously extracted.

II. PRINCIPLE AND SYSTEM

Fig. 1 shows the schematic diagram of the proposed lidar system. To achieve FMCW laser ranging, a chirped laser is used as the light source, in which an LFM lightwave is generated to detect targets. In the local transceiver, the LFM lightwave is first split by an optical coupler (OC). One part of the light is used as the local oscillator (LO), which can be expressed as

$$E_{LO} = A_{LO} \exp[j2\pi(f_c + f_0 + kt/2)t], \quad (1)$$

where A_{LO} is the amplitude of the optical field, f_c is the frequency of the optical carrier, and $f_0 + kt$ is the instantaneous frequency shift.

The other part of the lightwave is transmitted from the local transceiver, which is collected and amplified in the remote transceiver. The optical field can be given by

$$E_T = A_T \exp[j2\pi(f_c + f_0 + k(t - \tau)/2 + f_d)(t - \tau)], \quad (2)$$

where $\tau = R/c$ is the time delay of the optical signal, $f_d = v f_c/c$ is the optical DFS, A_T is the amplitude of the optical field, c is the speed of light, R and v are the range and the line-of-sight velocity of the remote transceiver, respectively. In the remote transceiver, the optical signal is coded by a digital baseband signal for the purpose of FSO communications, which is then transmitted back to the local transceiver.

Usually, the digital modulation for the reflected light can be achieved via amplitude modulation using a retro-modulator [20], [21], which is simulated using a Mach-Zehnder intensity modulator in the following proof-of-concept experiment. Therefore, the expression for a Mach-Zehnder intensity modulator is used here to describe the optical signals. The optical field reflected from the remote transceiver can be given by

$$E_R = A_R \cos\left(\frac{\pi DATA(t - 2\tau)}{2V_\pi} + \frac{\pi}{4}\right) \times \exp\left[j2\pi\left(f_c + f_0 + \frac{k}{2}(t - 2\tau) + 2f_d\right)(t - 2\tau)\right], \quad (3)$$

where A_R is the amplitude of the transmitted optical field, $DATA(t)$ is the digital baseband signal, and V_π is the half-wave voltage of the Mach-Zehnder modulator (MZM).

In the local transceiver, the reflected light is detected by a phase-diversity coherent optical receiver, which contains a 90-degree optical hybrid and two balanced photodetectors (BPDs). The two photocurrents from the two BPDs can be expressed as [22]

$$I_{PD1} = \eta \cos\left(\frac{\pi DATA(t - 2\tau)}{2V_\pi} + \frac{\pi}{4}\right) \times \cos[2\pi(f_R - 2f_d)t + \phi]$$

$$I_{PD2} = \eta \cos\left(\frac{\pi DATA(t - 2\tau)}{2V_\pi} + \frac{\pi}{4}\right) \times \sin[2\pi(f_R - 2f_d)t + \phi], \quad (4)$$

where $f_R = 2k\tau$ is the frequency related to the distance of the target, $\phi = 2\pi(2k\tau^2 - f_c - f_0 - 2f_d)$ is a constant phase, η is a constant coefficient. In a coherent lidar, only one photodetector is usually used. The carrier frequencies of the photocurrent of the photodetector (I_{PD1} or I_{PD2}) are varied depending on the distance and velocity of the target. If the carrier frequency $f_R - 2f_d$ is lower than the bit rate of the data, it is difficult to recover the digital baseband signal from the photocurrent.

To overcome this limit, in our proposed lidar system, a complex output signal is reformed by a digital signal processor (DSP), of which the signal I_{PD1} and I_{PD2} are the in-phase (I) and quadrature (Q) components, respectively. The complex output signal is given by

$$\mathbf{I}_{out} = I_{PD1} + jI_{PD2}$$

$$= \eta \cos\left(\frac{\pi DATA(t - 2\tau)}{2V_\pi} + \frac{\pi}{4}\right) \times \exp[j(2\pi(f_R - 2f_d)t + \phi)]. \quad (5)$$

A signal (I_1) can be obtained from the intensity of the complex signal, which is given by

$$I_1 = |\mathbf{I}_{out}|^2 \approx \eta^2 \left\{ 1 - \pi \frac{DATA(t - 2\tau)}{V_\pi} \right\}. \quad (6)$$

Meanwhile, the argument of the complex signal can also be extracted, which is expressed as

$$\Phi = \arg(\mathbf{I}_{out}) = 2\pi(f_R - 2f_d)t + \phi. \quad (7)$$

It should be noted that I_1 only carries the digital baseband signal and can be used to recover the communication data. The argument of the complex signal is proportional to the time (t). If an LFM signal with a triangular waveform is used, the argument of the complex signal can be expressed as

$$\Phi = \begin{cases} 2\pi(f_R - 2f_d)t + \phi, & \text{up-ramp} \\ 2\pi(f_R + 2f_d)t + \phi, & \text{down-ramp.} \end{cases} \quad (8)$$

The slopes of the Φ - t curve in the up-ramp and down-ramp sections are $2\pi(f_R - 2f_d)$ and $2\pi(f_R + 2f_d)$, respectively. The range and velocity of the target can be separately obtained from the sum and difference of the two different slopes.

III. EXPERIMENT AND DISCUSSIONS

A proof-of-concept experiment was carried out of which the schematic diagram is shown in Fig. 2. In the local transceiver, an LFM lightwave was generated by carrier-suppressed optical single-sideband (CS-OSSB) modulation. A lightwave from a 1550-nm narrow linewidth laser diode (LD, TeraXion

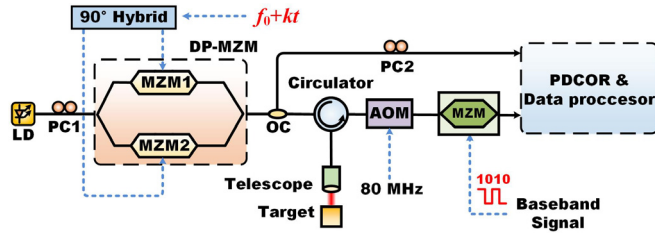


Fig. 2. Schematic diagram of the experiment system. The solid black lines and dashed blue lines are optical fibers and electrical cables, respectively. LD: laser diode; PC: polarization controller, DP-MZM: dual-parallel Mach-Zehnder modulator; OC: optical coupler, AOM: acousto-optic modulator.

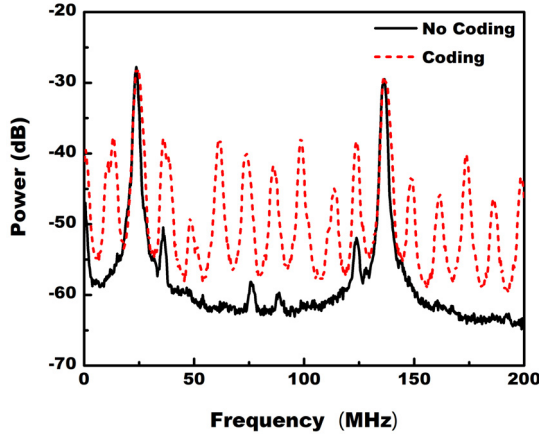


Fig. 3. The spectra of the de-chirped signals using a triangular waveform with and without digital coding. The pattern of the baseband signal is ‘11010010’ and the bit rate is 50 Mbps.

PS-NLL) was modulated by a dual-parallel Mach-Zehnder modulator (DP-MZM, Fujitsu FTM7961). A 7.5-12.5 GHz LFM signal with a triangular waveform and a period of $100 \mu\text{s}$ was generated by an arbitrary waveform generator (AWG, Tektronix AWG70001A). Using CS-OSSB modulation, only the +1st-order sideband existed in the modulated optical signal so that an LFM lightwave was finally generated. The LFM lightwave was then transmitted to the remote transceiver. In the proof-of-concept experiment, an MZM (Fujitsu FTM7938) was used to simulate a retro-modulator, by which the digital baseband signal was encoded on the reflected light. The digital signal was generated by a programmable pattern generator (PPG). Meanwhile, an 80-MHz acousto-optic modulator (AOM) was used to simulate a high-frequency optical DFS in the experiment system. Finally, the reflected light and the LO were sent to a phase-diversity coherent optical receiver (Fujitsu FIM24706) in the local transmitter. The output signals of the phase-diversity coherent optical receiver were simultaneously measured by a real-time oscilloscope (R&S, RTM1054) and off-line processed.

In a traditional coherent FMCW lidar, the digital baseband signal impacts the waveform of the lidar signal so that the spectrum will be changed. In Fig. 3, the spectrum of the de-chirped lidar signal (solid black line) shows two peaks, of which the range and velocity can be extracted. The signal-to-noise ratio (SNR) is around 22.5 dB, which corresponding to a distance accuracy of $\pm 0.022 \text{ m}$. However, the spectrum shows multiple peaks (dashed red line) if the lidar signal is coded with the digital signal. The SNR is reduced to

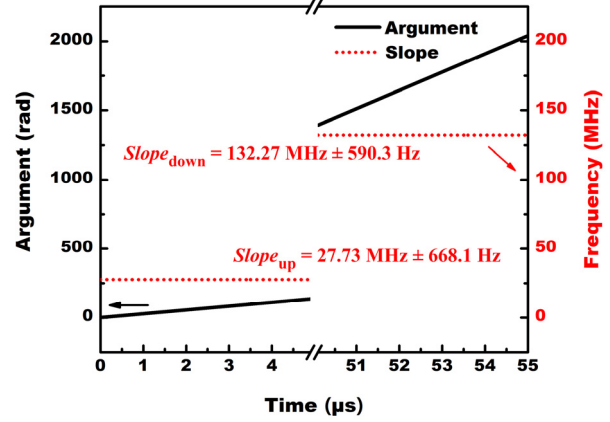


Fig. 4. The arguments (black solid line) and the slopes (red dotted line) calculated from I_{out} in the time slots of 0-5 μs and 50-55 μs . The values of the arguments and slopes are shown as the left and right axes, respectively.

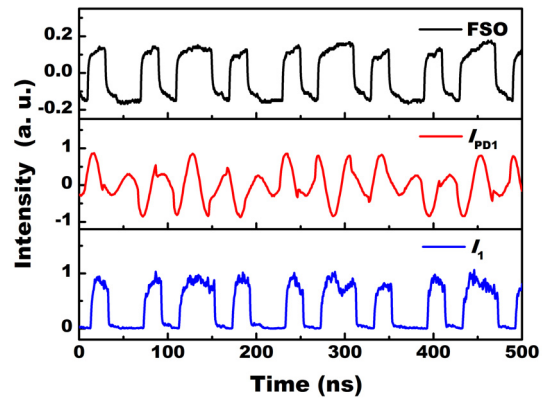


Fig. 5. The recovered baseband signals. Top: The signal obtained by the FSO communications. Middle: The signal recovered from I_{PD1} , which cannot be used to recover the baseband signal. Bottom: The baseband signal recovered from I_1 . The pattern of ‘11010010’. The bit rate is 50 Mbps.

9.7 dB, which results in a distance accuracy of $\pm 0.098 \text{ m}$. The accuracy is largely worsened due to the digital baseband signal. However, in our proposed system, the range and velocity are extracted from the argument of the complex output signal, while the digital signal only modulates the amplitude of the signal so that the effect of the digital signal can be largely reduced. Fig. 4 shows the calculated argument at different times (solid black lines). The pattern of the digital baseband signal is ‘11010010’ and the bit rate is 50 Mbps. The frequency is ramping up in 0-5 μs , while it is ramping down in 50-55 μs . The slopes of the $\Phi - t$ curve (dotted red lines) in the two sections are extracted by linear fitting, which are $27.73 \text{ MHz} \pm 668.1 \text{ Hz}$ and $132.27 \text{ MHz} \pm 590.3 \text{ Hz}$, respectively. The corresponding distance is $156.81 \pm 0.0019 \text{ m}$, of which the accuracy is largely enhanced due to the use of phase-derived ranging [23].

To demonstrate the downlink communication capability of the proposed lidar system, digital baseband signals are recovered and shown in Fig. 5. The patterns of these digital baseband signals are ‘11010010’ and the bit rate is 50 Mbps. For comparison, FSO communications are performed with a single-frequency optical carrier. The recovered signal is shown in the top subfigure of Fig. 5. But, in the FMCW coherent lidar, the de-chirped signal (I_{PD1}) is the carrier of the baseband signals, of which the frequency depends on the range

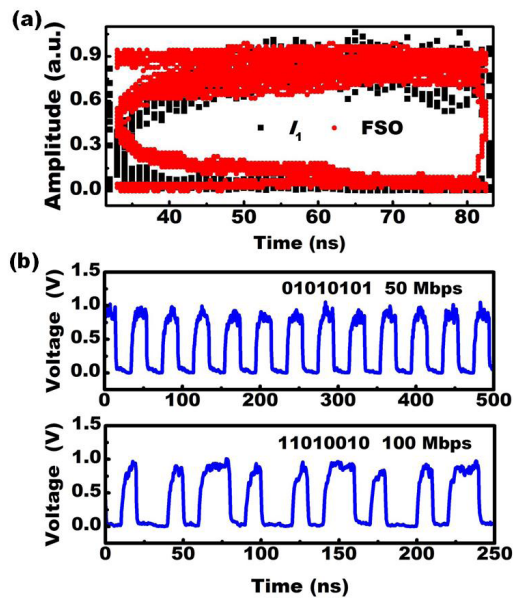


Fig. 6. (a) The eye-diagrams recovered from I_1 (black scatters) and the FSO communications (red scatters). (b) Different signals recovered by the proposed system. The patterns and the bit rates are shown as the legends in the figure.

and velocity of the target. If the frequency of I_{PD1} is lower than the bit rate, the communications cannot be achieved. In the middle subfigure of Fig. 5, the 50 Mbps baseband signal is difficult to be recovered since the frequency of I_{PD1} is 27.73 MHz.

In our proposed lidar system, the data can be recovered from the signal I_1 even though the bit rate is higher than the frequency of the de-chirped lidar signal, which is shown as the solid black line in the bottom subfigure of Fig. 5. Although the intensity of the signal shows large fluctuations when the code is “1”, it is very flat when the code is “0” which indicates a wide-open eye-diagram. The eye-diagrams recovered from I_1 (black scatters) and the FSO communications (red scatters) are shown in Fig. 6 (a). There is no obvious reduction of communication quality shown in the eye-diagram for the proposed system. Moreover, digital baseband signals with different patterns and bit rates are also encoded on the lidar signal. Fig. 6(b) shows the signals recovered from I_1 , which demonstrates that communications can always be achieved no matter whether the frequency of the de-chirped signal is higher than the bit rate or not.

IV. CONCLUSIONS

In conclusion, an FMCW lidar system with the downlink communications capability is proposed and demonstrated, in which the ranging, velocimetry, and FSO downlink communications are simultaneously achieved. In the remote transceiver, the LFM lightwave is coded with data and back-transmitted. A phase-diversity coherent optical receiver is used in the local transceiver to simultaneously extract the range, velocity, and communication data. The impact of the varied de-chirped frequency can be removed from the digital signal so that the communication quality is guaranteed. Meanwhile, the accuracy of the lidar is not worsened even when the lidar waveforms are significantly changed by the digital coding. The proposed system can be applied in the areas of navigation,

which require simultaneous laser ranging, laser velocimetry and FSO communications.

REFERENCES

- [1] C. A. Northend, R. C. Honey, and W. E. Evans, “Laser radar (Lidar) for meteorological observations,” *Rev. Sci. Instrum.*, vol. 37, no. 4, pp. 393–400, Apr. 1966.
- [2] V. Pasyonkov, M. Sadovnikov, V. Sumerin, and V. Shargorodskiy, “The concept and preliminary results of use of satellite laser ranging for GLONASS accuracy improvement,” presented at the 18th IWLR, Fujiyoshida, Japan, Nov. 2013.
- [3] R. C. Schnell *et al.*, “Lidar detection of leads in arctic sea ice,” *Nature*, vol. 339, no. 4, pp. 530–532, Jun. 1989.
- [4] R. H. Rasshofer and K. Gresser, “Automotive radar and lidar systems for next generation driver assistance functions,” *Adv. Radio Sci.*, vol. 3, pp. 205–209, May 2005.
- [5] H. Wang, B. Wang, B. Liu, X. Meng, and G. Yang, “Pedestrian recognition and tracking using 3D LiDAR for autonomous vehicle,” *Robot. Auto. Syst.*, vol. 88, pp. 71–78, Feb. 2017.
- [6] T. Sankey, J. Donager, J. McVay, and J. B. Sankey, “UAV lidar and hyperspectral fusion for forest monitoring in the southwestern USA,” *Remote Sens. Environ.*, vol. 195, pp. 30–43, Jun. 2017.
- [7] R. W. Wolcott and R. M. Eustice, “Fast LIDAR localization using multiresolution Gaussian mixture maps,” in *Proc. IEEE ICRA*, Seattle, WA, USA, May 2015, pp. 2814–2821.
- [8] A. Pfrunder, P. V. K. Borges, A. R. Romero, G. Catt, and A. Elfes, “Real-time autonomous ground vehicle navigation in heterogeneous environments using a 3D LiDAR,” in *Proc. IEEE/RSJ Int. Conf. Intell. Robots Syst. (IROS)*, Vancouver, BC, Canada, Sep. 2017, pp. 2601–2608.
- [9] V. W. Chan, “Free-space optical communications,” *J. Lightw. Technol.*, vol. 24, no. 12, pp. 4750–4762, Dec. 2006.
- [10] C. Tatkeu, P. Deloof, Y. Elhillali, A. Rivenq, and J. M. Rouvaen, “A cooperative radar system for collision avoidance and communications between vehicles,” in *Proc. IEEE Intell. Transp. Syst. Conf.*, Sep. 2006, pp. 1012–1016.
- [11] J. Choi, V. Va, N. Gonzalez-Prelcic, R. Daniels, C. R. Bhat, and R. W. Heath, “Millimeter-wave vehicular communication to support massive automotive sensing,” *IEEE Commun. Mag.*, vol. 54, no. 12, pp. 160–167, Dec. 2016.
- [12] S. Arnon and N. S. Kopeika, “Laser satellite communication network-vibration effect and possible solutions,” *Proc. IEEE*, vol. 85, no. 10, pp. 1646–1661, Oct. 1997.
- [13] A. Sutton, K. McKenzie, B. Ware, and D. A. Shaddock, “Laser ranging and communications for LISA,” *Opt. Express*, vol. 18, no. 20, p. 20759, Sep. 2010.
- [14] P. Feneyrou *et al.*, “Frequency-modulated multifunction lidar for anemometry, range finding, and velocimetry—1 theory and signal processing,” *Appl. Opt.*, vol. 56, no. 35, p. 9663, Dec. 2017.
- [15] S. Gao, M. O’Sullivan, and R. Hui, “Complex-optical-field lidar system for range and vector velocity measurement,” *Opt. Express*, vol. 20, no. 23, p. 25867, Nov. 2012.
- [16] P. A. M. Sandborn, N. Kaneda, Y.-K. Chen, and M. C. Wu, “Dual-sideband linear FMCW lidar with homodyne detection for application in 3D imaging,” in *Proc. Conf. Lasers Electro-Optics*, Sep. 2016, pp. 1–2.
- [17] C. F. Abari, A. T. Pedersen, and J. Mann, “An all-fiber image-reject homodyne coherent Doppler wind lidar,” *Opt. Express*, vol. 22, no. 21, p. 25880, Oct. 2014.
- [18] Z. Xu, K. Chen, H. Zhang, and S. Pan, “Multifunction lidar system based on polarization-division multiplexing,” *J. Lightw. Technol.*, vol. 37, no. 9, pp. 2000–2007, May 1, 2019.
- [19] K. Chen, H. Zhang, Z. Xu, and S. Pan, “FMCW lidar with communication capability using phase-diversity coherent detection,” in *Proc. 24th Optoelectron. Commun. Conf. (OECC) Int. Conf. Photon. Switching Comput. (PSC)*, Jul. 2019, pp. 1–3.
- [20] M. Achour, “Free-space optical communication by retro-modulation: Concept, technologies, and challenges,” *Proc. SPIE*, vol. 5614, pp. 52–63, Dec. 2004.
- [21] B. Born, I. R. Hristovski, S. Geoffroy-Gagnon, and J. F. Holzman, “All-optical retro-modulation for free-space optical communication,” *Opt. Express*, vol. 26, no. 4, p. 5031, Feb. 2018.
- [22] Z. Xu, H. Zhang, K. Chen, D. Zhu, and S. Pan, “FMCW lidar using phase-diversity coherent detection to avoid signal aliasing,” *IEEE Photon. Technol. Lett.*, vol. 31, no. 22, pp. 1822–1825, Nov. 15, 2019.
- [23] S. Li *et al.*, “Optical fiber transfer delay measurement based on phase-derived ranging,” *IEEE Photon. Technol. Lett.*, vol. 31, no. 16, pp. 1351–1354, Aug. 15, 2019.